Postprint of: Ogurtsov S., Koziel S.: On Alternative Approaches to Design of Corporate Feeds for Low-Sidelobe Microstrip Linear Arrays, IEEE TRANSACTIONS ON ANTENNAS AND PROPAGATION, Vol. 66, iss. 7 (2018), pp. 3781-3786, DOI: 10.1109/TAP.2018.2823915

On Alternative Approaches to Design of Corporate Feeds for Low-Sidelobe Microstrip Linear Arrays

Stanislav Ogurtsov and Slawomir Koziel

***Abstract*—Two design approaches, illustrated by simulations and measurements, aiming at a systematic computer-aided design of printed circuit feeds for low-sidelobe microstrip antenna arrays are described. The novelty of these approaches resides in identification of the optimal feed architectures with subsequent simulation-based optimization of the feed and array aperture dimensions. In this work, we consider microstrip corporate feeds realizing nonuniform amplitude excitation of linear arrays of microstrip patch antennas. Two types of the microstrip corporate feeds are considered: with equal power split junctions, and with unequal power split junctions. For each feed type, we identify candidate prototypes of feed architectures using numerical optimization of the corresponding fast feed models. Subsequently, the architectures are implemented as microstrip sub-circuits within the antenna array electromagnetic (EM) models. For the sake of comparison, the antenna array circuits are defined with the same linear array of microstrip patch antennas featuring the half-wavelength element spacing, and implemented on the same microstrip substrates. Finally, the EM models are tuned—using simulation-based optimization techniques—to ensure an appropriate input reflection coefficient and minimum sidelobe levels. Selected optimal designs of antenna array circuits with twelve microstrip patches and different feeds are manufactured and measured.**

***Index Terms*—Antenna array feeds, antenna measurements, computer aided design, corporate feeds, linear antenna arrays, microstrip antenna arrays, printed circuit feeds, sidelobe levels, radiation patterns, optimization**

I. INTRODUCTION

Realization of low sidelobes becomes challenging for printed circuit antenna arrays, microstrip antenna arrays in particular, for sidelobe levels lower than –20 dB. Factors affecting realizable sidelobe levels of microstrip antenna arrays were studied [1,2]. Corporate feeds with unequal power split junctions can realize nonuniform amplitude excitations required for low-sidelobe antenna arrays. Designs of such feeds have been demonstrated for printed [3–9] and waveguide [10] circuits. Wilkinson and branch-line dividers can improve feeds' performance at the expense of complexity [9,11,12]. Series feeds for microstrip antenna arrays can be more economical in terms of feed footprints and also realize low sidelobe patterns to certain extend [13,14]. On the other hand, corporate feeds allow for better control of amplitude and phase of radiating elements, thereby allowing design approaches developed for fixed beam arrays be extendable for phased, multibeam, and shaped-beam antenna arrays [15,16].

A systematic approach to design of corporate feeds for broadside microstrip linear antenna arrays was demonstrated [17] for Chebyshev excitation. The approach identifies the candidate feed architectures and corresponding sets of power split ratios. However, low sidelobe levels (SLLs) of the entire microstrip antenna array circuits, with the corporate feeds built with unequal power split T-junctions, can be challenging to realize in practice due to manufacturing non-idealities, interactions within the circuit, radiation from the feed, as well as signal emission to the substrates.

Another approach to design of corporate feeds for low sidelobe linear arrays has been proposed in [18], where, for a given linear array aperture with an even number of radiators, only equal power split T-junctions were used. The adopted T-junction configuration is with a lower impedance section of a matching section at the input. Feed architectures with the lowest SLL, and the simplest routing were being detected.

The approaches of [17] and [18] include identification of the optimal feed architectures with subsequent simulation-based optimization of the feed and radiating aperture dimensions. To our understanding, these approaches can be useful as alternatives for design of printed-circuit low-sidelobe linear antenna arrays where the post-manufacturing tuning of the radiating aperture and the feed is limited or even impossible.

In this paper we outline the two approaches to CF design, describe their similarities and differences. Numerical results and measurements are presented for 5.8 GHz twelve element microstrip linear arrays. We compare the simulated and measured reflection coefficients and radiation patterns, including the realized SLLs, for selected manufactured designs obtained with the two approaches.

II. CORPORATE FEED DESIGN APPROACHES

We consider symmetrical broadside linear antenna arrays with an even number of radiators, as depicted in Fig. 1(a), producing the sum pattern. The arrays should be implemented with microstrip patch antennas. Design task includes minimization of the SLL and the reflection coefficient at the feed input. The feeds are designed with simple T-junctions. The T-junctions should be made matched at the input and allow unequal power split for Approach I [17], as the T-junctions drawn in Fig. 2(a) and (b). For Approach II [18] only equal power split T-junctions will be adopted, as T-junctions in Fig. 2(c). For the sake of clarity the results will be presented for 5.8 GHz twelve element linear antenna arrays with half-wavelength spacing.

A. Architecture Selection and Optimization with Approach I

First, we searched for feed architectures realizing Chebyshev excitations for twelve element arrays with the –30 dB and –35 SLLs [19]. To avoid too narrow microstrip sections in the subsequent implementation of T-junctions, the lower and upper bounds for the power split were set to 0.33 and 0.67, respectively. Optimization of the fast feed models [17] has been implemented in Matlab [20]. Two architectures, most accurately approximating the Chebyshev excitations, are shown in Fig. 3(a). Because of the symmetry, only halves of the feeds are shown in Fig. 3(a). The central junction of the feeds is for equal power split and not shown in Fig. 3.

Next, the junctions of the best feeds were implemented in CST MWS [21] with microstrip T-junctions residing on the 0.762 mm RF-35 laminate [22]. The line impedance of inputs and outputs is 50 ohms. The junctions were tuned for the required power splits and matching at the input (denoted with 0s in Fig. 2). Numerical optimization of EM models of the junctions was applied for tuning. Because of a low-dimensionality of the junction problem, gradient-based optimization embedded in the trust-region framework was utilized [24]. The primary objective was minimization of the reflection coefficient at 5.8 GHz. Power splits were controlled using the penalty function approach [25].

Further, the feeds were implemented as microstrip circuits comprising

The manuscript was submitted on March 5, 2018.

This work was partially supported by the Icelandic Centre for Research (RANNIS) under RANNIS Grant 174114051.

S. Ogurtsov and S. Koziel are with Engineering Optimization & Modeling Center, Reykjavik University, 101 Reykjavik, Iceland (emails: stanislav@ru.is; koziels@ru.is). S. Koziel is also with the Faculty of Electronics, Telecommunications and Informatics, Gdansk University of Technology, 80-233 Gdansk, Poland.

This article has been accepted for publication in a future issue of this journal, but has not been fully edited. Content may change prior to final publication. Citation information: DOI 10.1109/TAP.2018.2823915, IEEE Transactions on Antennas and Propagation

individually optimized T-junctions. Based on the simulated transmission parameters of the feeds the geometrical lengths from the common input to the ground plane slots of all antennas were corrected to have the transmission parameters all in phase. The uncorrected feeds had the 12 degree spread of phase shifts.

Finally, the feed was included in the circuit comprising the feed, the array aperture, and an SMA connector [26]. The aperture is on a 1.574 mm TLP-5 substrate [27] and described in Section IIC. The entire circuit was validated with high fidelity EM simulations. Figure 4 outlines the entire design flow with Approach I.

B. Architecture Selection and Optimization with Approach II

Here we utilized T-junctions of the equal power split with a matching section at the input as shown in Fig. 2(c). Then the feed architectures as those outlined in Fig 3 realize certain nonuniform excitation [18]. The array factor served for identification of the architectures with reduces SLLs [18].

At the next stage, the architectures with the lowest expected SLLs, depicted in Fig. 3(b), were implemented using CST MWS in the aperture-feed integrated microstrip circuits. Geometrical lengths from the common input to the ground plane slots of all antennas are set to be equal at the initial design. EM-based optimization were applied to the EM models of the entire integrated circuits, There were 24 design variables (controlling dimensions of the antennas and the feed) in the EM model with the feed with element levels [2 2 3 3 3 3] and 26 variables with the feed with levels [2 2 2 3 4 4]. A one-side array with element levels [2 2 3 3 3 3], was also optimized for comparison. Figure 5 outlines the Approach II design flow.

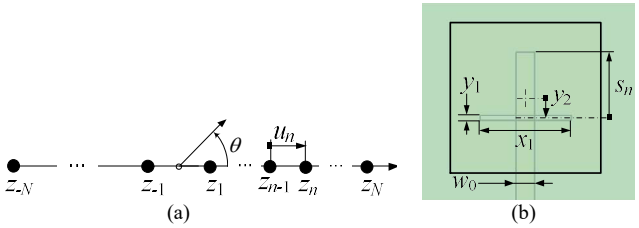

Fig. 1. Linear array aperture: (a) an aperture with symmetrical amplitudes and spacings; (b) an array element, a microstrip antenna energized through a ground plane slot.

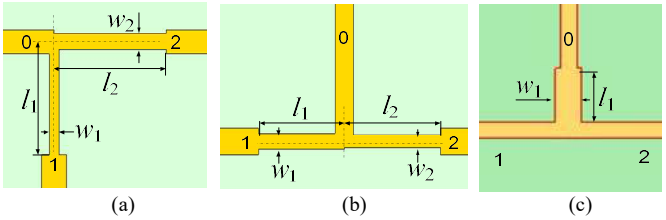

Fig. 2. T-junctions: (a) and (b) used with Approach I for unequal power splits; (c) used with Approach II for equal power split.

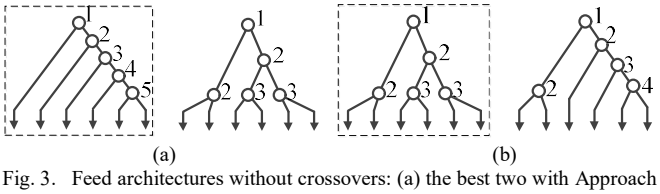

Fig. 3. Feed architectures without crossovers: (a) the best two with Approach I for the –35 dB Chebyshev excitation, where the one marked with the dashed-line box, is the best also for the –30 dB SLL Chebyshev excitation; (b) the best two architectures with Approach II with element levels [2 2 3 3 3] and [2 2 2 3 4 4] where the one marked with the dashed-line box is the best (–16.5 dB of the array factor SLL) for half-wavelength spacings.

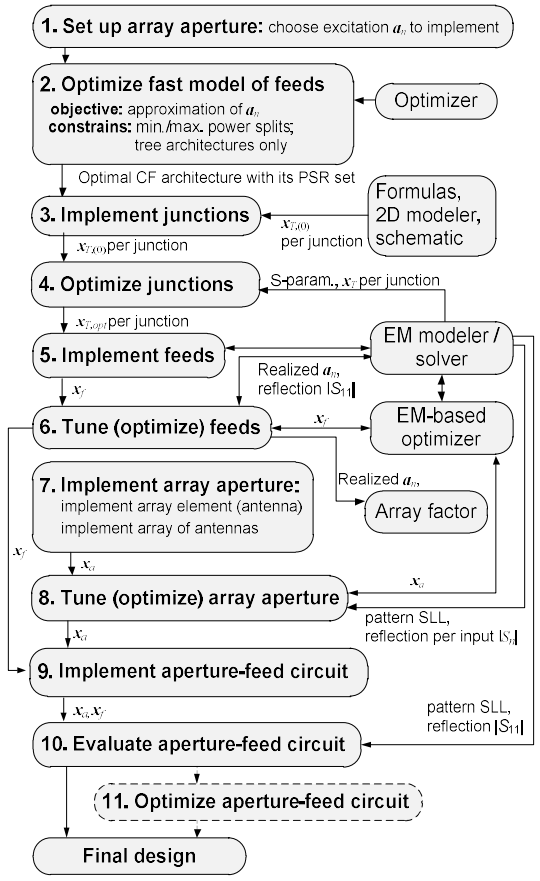

Fig. 4. Design process with Approach I where $\boldsymbol{x}_T$ is the vector of design variables per junction, $\boldsymbol{x}_f$ is the vector of the feed design variables, $\boldsymbol{x}_a$ is the vector of the aperture design variables.

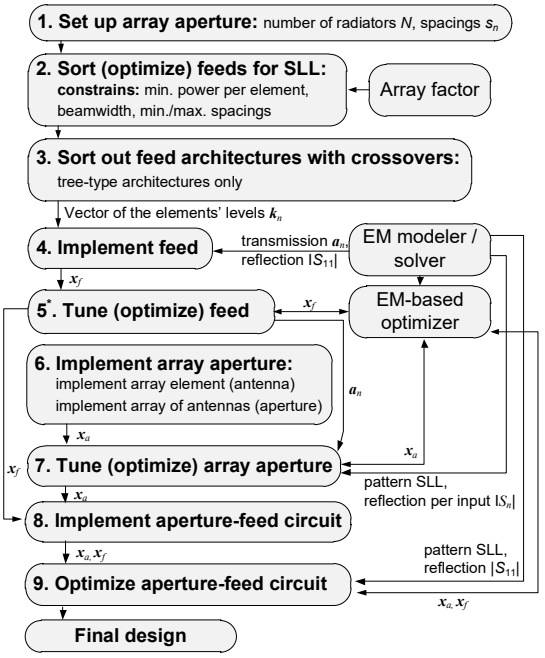

Fig. 5. Design process with Approach II where $\boldsymbol{x}_f$ is the vector of the feed design variables, $\boldsymbol{x}_a$ is the vector of the aperture design variables (including those of the array element (antenna). In this work, Step 5 (optimization of the feed) was implementd within the final Step 9 (EM-based optimization of the entire circuit).

This article has been accepted for publication in a future issue of this journal, but has not been fully edited. Content may change prior to final publication. Citation information: DOI 10.1109/TAP.2018.2823915, IEEE Transactions on Antennas and Propagation

C. *Modelling and Optimization of Antenna Array Apertures*

Four apertures consisting of twelve half-wave spaced linearly polarized 5.8 GHz microstrip patch antennas operating at the dominant TM_{010} mode [15] have been designed and the realized arrays are shown in Figs. 6-9. Figs. 6-8 are designs based on Approach II while Fig. 9 is a design based on Approach I. Fig. 7 is a single-layer design where the antenna elements and the feed structure are coplanar. The other three designs are two-layer structures. The antenna layout for the two-layer circuit is depicted in Fig. 1(b). Antenna dimensions are parametrized. Antenna inputs continue the feed. Lengths of the open-end microstrip sections, s_n, are element-specific. The line impedance of the inputs is 50 ohms. Before being connected to a particular feed in the EM model, the apertures had been tuned for 5.8 GHz using simulation-based optimization [28]. Aperture set up and optimization within Approach I are depicted as items 1, 7, and 8 in Fig. 4, and within Approach II are depicted as items 1, 6, and 7 in Fig. 5.

D. *Realized Design Processes with Approaches I and II*

The process of Approach I (outlined in Fig. 4) comprises more steps per design and optimization of the feed than that of Approach II (outlined in Fig. 5). This is due to a more demanding task imposed on the feed built in Approach I with unequal split junctions. At the same time, because of the lower dimensionality of the design problem with Approach II utilizing equal split T-junctions, EM-optimization of the feed (Step 9 in Fig. 5) energizing the antennas had been carried out.

III. Design Validation

Layouts of the circuits were created from the EM-tuned and optimized designs. Photographs of the manufactured designs are shown in Fig. 6 through 9. Nylon bolts fix the dielectric layers of all two-side designs. All circuits are with 18 μm copper metallization. The circuits were measured in the anechoic chamber of Reykjavik University. The measured responses are shown in Figs. 10 through 14. Summary of the patterns at 5.8 GHz is given with Table I.

IV. Discussion and Conclusions

Measured and simulated results are consistent according to Figs. 10—13 and Table I. Moreover, the measured and simulated SLLs of

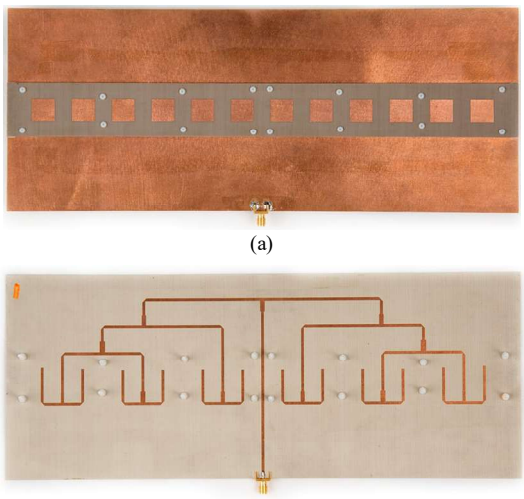

(a)

(b)

Fig. 6. Photographs of the 5.8 GHz 12-element microstrip array with the element levels [2 2 3 3 3 3]: (a) radiating aperture on two layers of TLP-5 (nominal thickness 1.574 mm in total). The TLP-5 layers are 329 mm × 35 mm. Microstrip patches are 14.85 mm by 14.85 mm; (b) feed on the 0.762 mm RF-35 layer with equal power split T-junctions. Ratiating elements are energized through ground plane slots. The RF-35 layer and the ground plane is 329 mm × 133 mm.

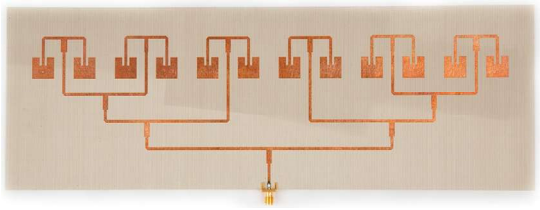

Fig. 7. Photograph of the 5.8 GHz 12-element microstrip array with the element levels [2 2 3 3 3 3]: one side realization on the 0.762 mm thick RF-35 layer. The microstrip RF-35 layer is 333 mm × 117 mm. The feed is with equal power split T-junctions. Microstrip patches are 13.74 mm by 13.80 mm.

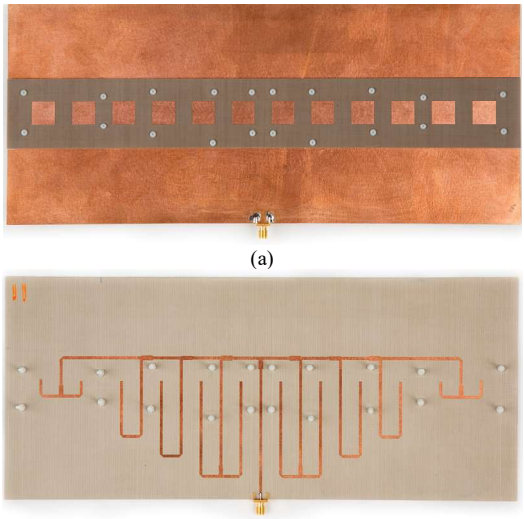

(a)

(b)

Fig. 8. Photographs of the 5.8 GHz 12-element microstrip array with the element levels [2 2 2 3 4 4]: (a) radiating aperture on two layers of TLP-5 (nominal thickness 1.574 mm in total). The TLP-5 layers are 329 mm × 45 mm. Microstrip patches are 14.85 mm by 14.85 mm; (b) feed on the 0.762 mm RF-35 layer with equal power split T-junctions. Ratiating elements are energized trough ground plane slots. The RF-35 layer and the ground plane is 329 mm × 145 mm.

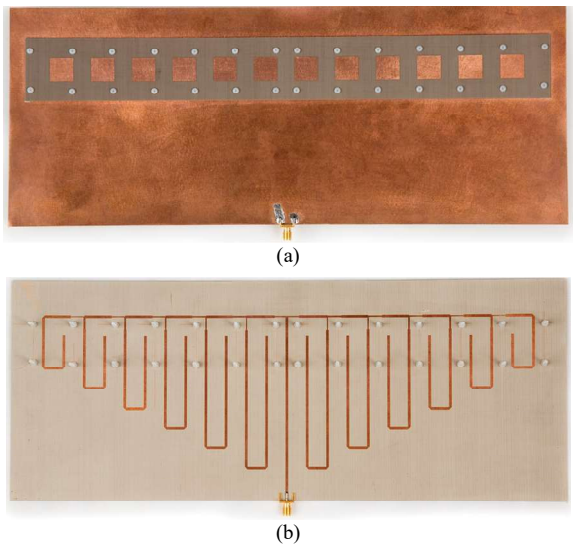

(a)

(b)

Fig. 9. Photographs of the 5.8 GHz 12-element array implementing the –30 dB SLL Chebyshev taper: (a) radiating aperture on two layers of TLP-5 (nominal thickness 1.574 mm in total). The TLP-5 layers are 330 mm × 40 mm. Microstrip patches are 14.85 mm by 14.85 mm; (b) realization of the feed architecture on the 0.762 mm RF-35 layer with unequal power split T-junctions. The RF-35 layer and the ground plane is 350 mm × 140 mm.

This article has been accepted for publication in a future issue of this journal, but has not been fully edited. Content may change prior to final publication. Citation information: DOI 10.1109/TAP.2018.2823915, IEEE Transactions on Antennas and Propagation

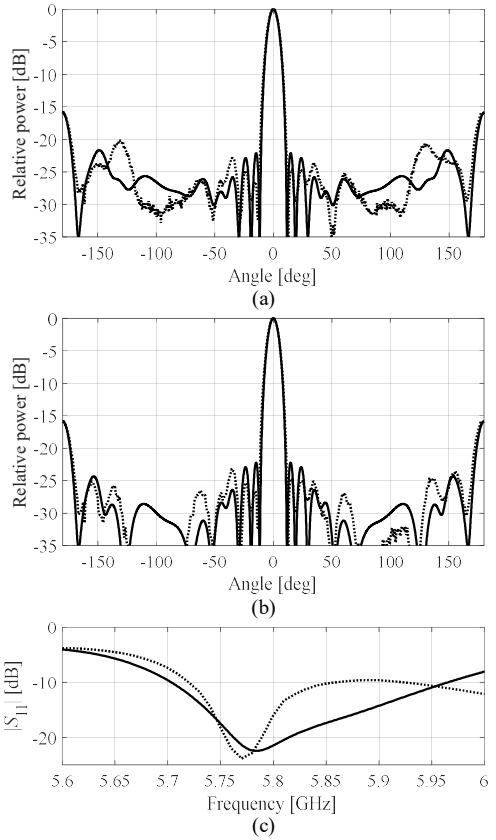

Fig. 10. Measured (···) and simulated (—) array of Fig. 6: H-plane (a) total (x-pol included), and (b) co-pol patterns at 5.8 GHz; (c) reflection coefficient.

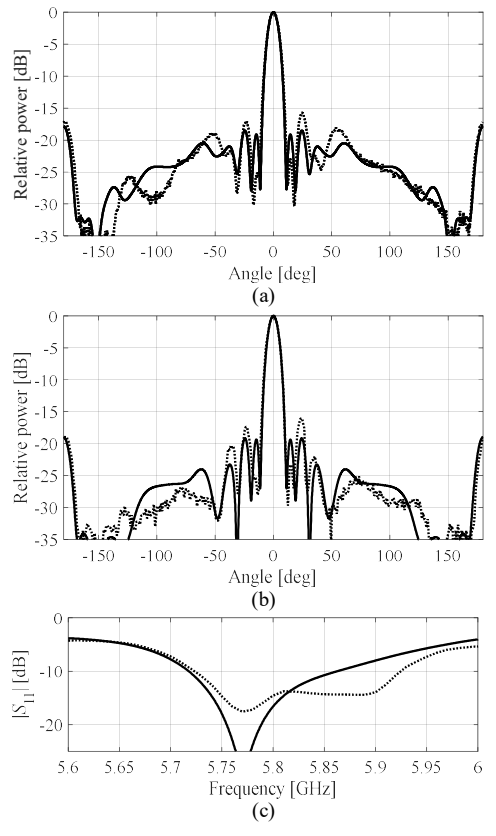

Fig. 11. Measured (···) and simulated (—) array of Fig. 7: H-plane (a) total (x-pol included), and (b) co-pol patterns at 5.8 GHz; (c) reflection coefficient.

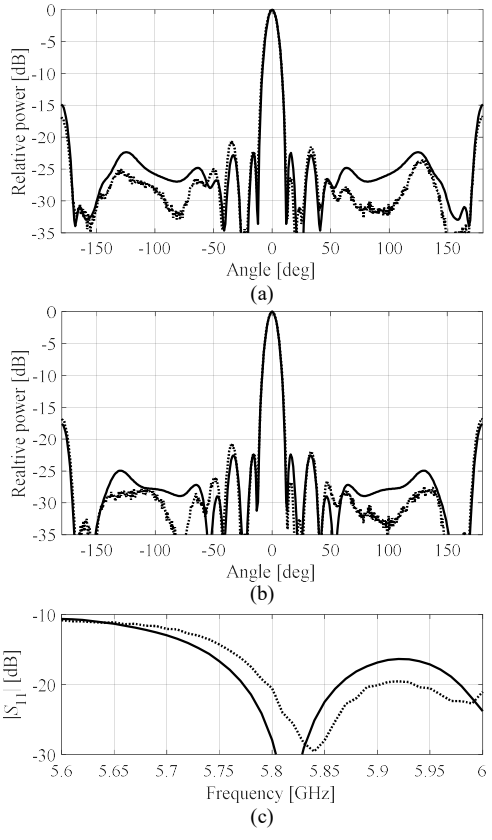

Fig. 12. Measured (···) and simulated (—) array of Fig. 8: H-plane (a) total (x-pol included), and (b) co-pol patterns at 5.8 GHz; (c) reflection coefficient.

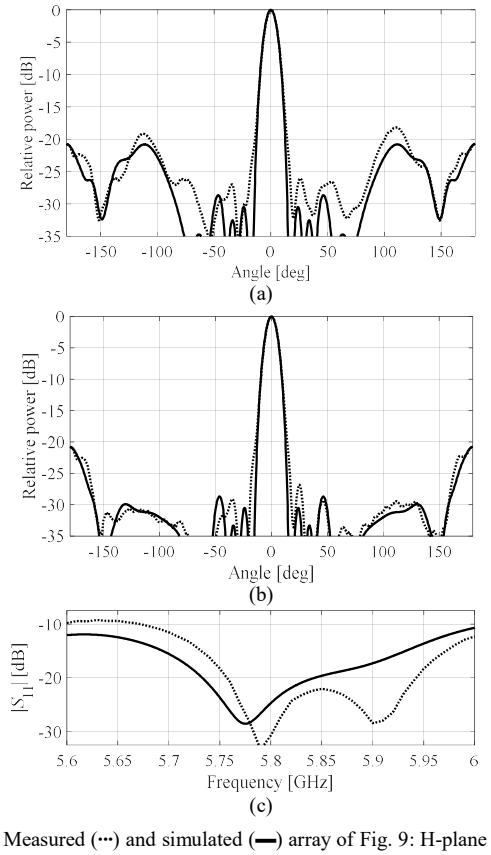

Fig. 13. Measured (···) and simulated (—) array of Fig. 9: H-plane (a) total (x-pol included), and (b) co-pol patterns at 5.8 GHz; (c) reflection coefficient.

This article has been accepted for publication in a future issue of this journal, but has not been fully edited. Content may change prior to final publication. Citation information: DOI 10.1109/TAP.2018.2823915, IEEE Transactions on Antennas and Propagation

the two-side designs (Figs. 10 and 12), which have been obtained with Approach II using EM optimization of entire circuits, are significantly lower than their SLL estimated using their fast models [18]. For instance, the design of Fig. 10 shows the measured SLL of –22.8 dB versus –16.5 dB estimated with the array factor and the element pattern. Similar improvement is obtained for the design of Fig. 8.

The measured patterns of the one layer array are shown in Fig. 11. The measured SLL of about –16 dB is close to the SLL predicted using the fast model before EM optimization. However, the EM simulated pattern and reflection coefficient have been significantly improved relative to those of the initial design, in –3 dB and –5 dB at 5.8 GHz, respectively. The higher SLL of this array, in comparison to the SLL shown in Fig. 10, as well as the inaccurate prediction of the array factor model for this array are, in a significant part, because of the radiation from the feed in the forward direction (not accounted for by the array factor model). Thus, the simulated and measured responses justify the use of EM-based optimization at the final stage of the Approach II design process.

The measured and simulated H-plane patterns of the design implementing the –30 dB Chebyshev taper using Approach I is shown in Fig. 13. Figure 13 shows that the increased SLL and back-lobes of the measured H-plane total power pattern are due to the cross-pol radiation which is mostly emitted by the feed according to our studies. According to our experiments, the array assembly inaccuracy as well as mechanical deformation (e.g., slight bending of the aperture and the feed) may significantly contribute to broadening of the measured main lobe for relative power below –20 dB. As an extension of this work the above issues should be solved using EM optimization of the entire circuit within Approach I as well as with application of absorbing materials.

The measured SLLs within [–90, 90] degree of the H-plane from 5.6 to 6.0 GHz are shown in Fig. 14 where the design implementing the –30 dB SLL Chebyshev taper shows the lowest SLL in overal in comparizon with other designs. At the same time, the SLL of this design is close to the SLL of the design shown in Fig. 6 at frequencies about 5.75 GHz. Thus, Approach II (with equal split junctions) can be a reliable option for low-sidelobe antenna arrays unless ultralow sidelobes are required.

TABLE I
H-PLANE RADIATION PATTERNS AT 5.8 GHZ

Design of Fig.	SLL [dB] in [-90°,90°]	Co-pol. SLL [dB] in [-90°,90°]	Front-to-Back Ratio [dB]	HPBW [Deg]
	Meas., Sim.	*Meas., Sim.*	*Meas., Sim.*	*Meas., Sim.*
6	−22.9,−22.1	−23.2,−22.2	15.8,15.8	−9.8,−9.4
7	−15.7,−18.5	−16.0,−18.6	17.0,17.8	−9.6,−9.3
8	−20.6,−22.5	−22.7,−22.5	16.9,14.9	−10.1,−9.8
9	−24.2, −26.8; −26.0[a], −28.7[a]	−26.8,−28.7	20.6,20.7 18.2[b],20.7[b]	−10.7,−10.8

[a] Measured and simulated SLL in [-75°,85°]
[b] Measured and simulated highest back-lobes

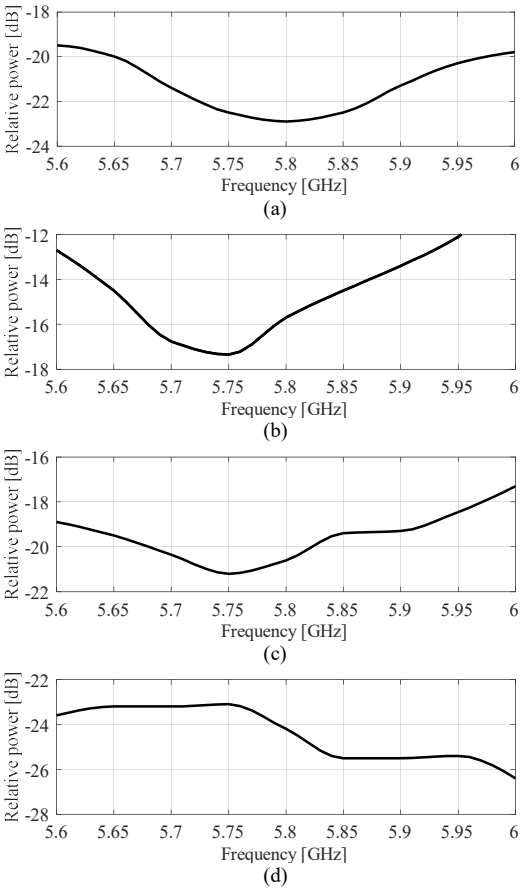

Fig. 14. Measured SLL within the [-90,90] degree sector of the H-plane: (a) array of Fig. 6; (b) array of Fig. 7; (c) array of Fig. 8; (d) array of Fig. 9.

REFERENCES

[1] D.M. Pozar, B. Kaufman, "Design considerations for low sidelobe microstrip arrays," IEEE Trans. Antennas Propagat., vol. 38, no.8, pp. 1176-1185, Aug. 1990.

[2] Y.-W. Kang, D.M. Pozar, "Correction of error in reduced sidelobe synthesis due to mutual coupling," IEEE Trans. Antennas Propagat., vol. AP-33, no.9, pp. 11025-1028, Sep. 1985.

[3] P.S. Hall, J.R. James, "Design of microstrip antenna feeds. Part 2: design and performance limitations of triplate corporate feeds," IEE Proc. H Microw. Opt. Antennas, 1981,vol. 128, iss. 1, pp. 26-34.

[4] P.S. Hall, C.M. Hall, "Coplanar corporate feed effects in microstrip patch array design," IEE Proceedings H - Microwaves, Antennas and Propagation, 1988, vol. 135, iss. 3, pp. 180-186, 1988.

[5] E. Levine, S., Shtrikman, "Optimal designs of corporate-feed printed arrays adapted to a given aperture," Proc. The Sixteenth Conference of Electrical and Electronics Engineers in Israel, Tel-Aviv, Israel, March 1989, pp. 1-4..

[6] E. Levine, G. Malamud, S. Shtrikman, D. Treves, "A study of microstrip array antennas with the feed network," IEEE Transactions on Antennas and Propagation, vol. 37, iss. 4, pp. 426-434, 1989.

[7] T.-S. Horng, N.G. Alexopoulos, "Corporate feed design for microstrip arrays," IEEE Trans. Ant. Propag., vol. 41, iss. 12, pp. 1615-1624, 1993.

[8] J. Wang, J. Litva, "Design study of a low sidelobe microstrip antenna array and feed network," Digest AP-S Int. Symposium, 1989, pp. 882-885.

[9] F.-C. Chen, H.-T. Hu, R.-S. Li, Q.-X. Chu, and M.J. Lancaster, "Design of filtering microstrip antenna array with reduced sidelobe level," IEEE Trans. Antennas Propagat., vol. 65, no. 2, pp.903-908, 2017.

[10] T.K. Anthony, A.I. Zaghloul, "Designing a 32 element array at 76GHz with a 33dB taylor distribution in waveguide for a radar system," Proc. 2009 IEEE Antennas and Propagation Society Int. Symposium, North Charleston, SC, USA, June 2009, pp. 1-4.

[11] P. Rigoland, M., Drissi, C., Terret, P., Gadenne, "Wide-band planar arrays for radar applications," Proc. IEEE Int. Symp. Phased Array Systems and Technology, Boston, MA, USA, Oct. 1996, pp. 163-167.
[12] Y.-J. Hu, W.-P. Ding, W.-Q. Cao, "Broadband circularly polarized microstrip antenna array using sequentially rotated technique," IEEE Antennas Wireless Prop. Lett., vol. 10, pp. 1358-1361, 2011.
[13] J. Yin, Q. Wu, C. Yu, H. Wang, W. Hong, "Low-sidelobe-level series-fed microstrip antenna array of unequal interelement spacing," IEEE Antennas and Wireless Propagation Letters, vol. 16, pp. 1695-1698, 2017.
[14] S. Afoakwa, Y.-B. Jung, "Wideband microstrip comb-line linear array antenna using stubbed-element technique for high sidelobe suppression," IEEE Trans. Antennas Propagat., vol. 65, no. 10, pp. 5190-5199, 2017.
[15] C.A. Balanis, Antenna Theory: Analysis and Design, 3rd ed., Wiley-Interschience, 2005.
[16] R.C. Hansen, Phased array antennas, 2nd ed.,Wiley, 2009.
[17] S. Koziel, S.Ogurtsov, "On systematic design of corporate feeds for Chebyshev microstrip linear arrays," 2017 IEEE Antennas Propagat. Society Int. Symposium, San Diego, CA, USA, July 2017, pp. 1-2.
[18] S.Ogurtsov, S. Koziel, "Systematic approach to sidelobe reduction in linear antenna arrays though corporate-feed-controlled excitation," IET Microwaves, Antennas & Propagation, vol. 11, iss., 6, pp. 779-786, 2017.
[19] R.J. Stegen, "Excitation coefficients and beamwidths of Tschebyscheff arrays," Proceedings of IRE, vol. 41, iss. 11, pp. 1671-1674, 1953.
[20] Matlab R2013a, The MathWorks, Inc., 2013, Natick, MA, USA.
[21] CST Microwave Studio, ver. 2016, CST AG, Darmstadt, Germany.
[22] Taconic RF-35, Technical data sheet, Taconic Int. Ltd, Ireland, 2016.
[23] D.M. Pozar, "The T-junction power divider", in D.M. Pozar, Microwave Engineering, Addison-Wesley Publ. Company, 1993, pp. 391-394.
[24] A.R. Conn, N.I.M. Gould, P.L. Toint, Trust Region Methods, MPS-SIAM Series on Optimization, 2000.
[25] S. Koziel and S. Ogurtsov, Antenna design by simulation-driven optimization. Surrogate-based approach, Springer, 2014.
[26] SMA 50 Ohm Connector, part. number 142-0701-881(A), Data Sheet, Chinch Connectivity Solutions, Waseca, MN, USA.
[27] Taconic TLP, Technical data sheet, Taconic Int. Ltd, Ireland, 2013
[28] S. Koziel, S. Ogurtsov, W. Zieniutycz, L. Sorokosz, "Simulation-Driven Design of Microstrip Antenna Subarrays," IEEE Transactions on Antennas and Propagation, vol. 62, iss. 7, pp. 3584-3591, 2014.